Nuclear Materials and Energy 000 (2016) 1–6

Contents lists available at ScienceDirect

Nuclear Materials and Energy

journal homepage: www.elsevier.com/locate/nme

Identification of intermittent transport in the scrape-off layer of MAST through high speed imaging

N.R. Walkden[a,*], F. Militello[a], J. Harrison[a], T. Farley[a,b], S. Silburn[a], J. Young[c]

[a] CCFE, Culham Science Center, Abingdon, Oxfordshire, OX14 3DB, UK
[b] Department of Electrical Engineering and Electronics, University of Liverpool, Brownlow Hill, Liverpool, L69 3GJ, UK
[c] University of Manchester, School of Physics and Astronomy, Oxford Road, Manchester, M13 9PL, UK

ARTICLE INFO

Article history:
Received 7 July 2016
Revised 23 September 2016
Accepted 17 October 2016
Available online xxx

ABSTRACT

Using footage from high speed movies taken of the boundary plasma in the Mega Amp Spherical Tokamak (MAST) general properties of filaments are inferred through statistical moments. Filaments are observed up to and beyond the $\psi_N = 1.5$ flux surface which, in single null configurations, lies well beyond the secondary separatrix and leads to filaments observed > 30 cm from the top of the plasma. In the divertor filaments are observed to connect through to the target, however a quiescent region is observed close to the X-point where no coherent filaments are identified. This region coincides with a sharp rise in the integrated magnetic shear which may change the nature of the filament cross-section.

1. Introduction

The scrape-off layer region (SOL) of a tokamak plasma is the interface between the hot plasma core and cold material surfaces [1]. In future reactor scale machines such as ITER [2] and DEMO [3] protection of plasma facing components will be a primary concern with any excessive damaging requiring repair and ultimately limiting operation of the machine. In order to predict the particle and heat loading onto these material surfaces it is essential that a proper understanding of the transport process in the SOL is developed. It is well known that the relationship between fluxes and gradients in the cross-field direction within the SOL is non-local [4]. Instead particle and heat transport can be mediated through the intermittent ejection and propagation of meso-scale coherent field aligned plasma objects known as filaments. Filaments have been observed in many tokamaks [5–7], as well as many other magnetically confined plasma devices [8,9], making them ubiquitous to the SOL of magnetically confined plasmas [10]. Recent forward modeling of heat flux [11] and particle flux [12] to the MAST divertor target suggests that the formation of SOL profiles at the divertor can be fully reconciled with experimental measurements through transport induced by filaments [11]. Furthermore filaments can carry hot ions towards the first-wall of the machine [13] and present a risk of damage to many plasma facing components (PFCs) in the tokamak. Consideration of these factors makes the task of understanding the production and propagation of filaments critical.

High speed imaging has been used in the past to identify filaments passively via wide angle viewing [5] or actively through the gas-puff imaging technique [6]. By being both inherently 2D in nature, and sampled at a high frequency both the geometry and motion of filaments can be measured using these techniques. In order to distill the multitude of information available from these movies this paper presents an analysis of the pixel-wise statistical moments of the movie from two different camera views of the MAST vessel. The analysis has been carried out for MAST L-mode plasmas in both the double-null (DND) and single-null (SND) magnetic configurations. This paper is organized as follows: Section 2 describes the setup of the camera used to produce the movies analysed and provides some identifiers to orient to the movie perspective. Section 3 presents statistical analysis of a DND and an SND plasma in the main chamber view. Section 4 presents analysis of the divertor view before section 5 summarizes.

2. Camera setup

The measurements presented in this paper were obtained with an unfiltered PHOTRON SA1 camera with two alternative tangential views into the MAST vessel. The viewing geometry of the camera in both the 'main chamber' and 'divertor' setup are shown in Fig. 1. The frame-rate, pixel resolution and exposure time used

* Corresponding author.
E-mail address: nick.walkden@ukaea.uk (N.R. Walkden).

http://dx.doi.org/10.1016/j.nme.2016.10.024

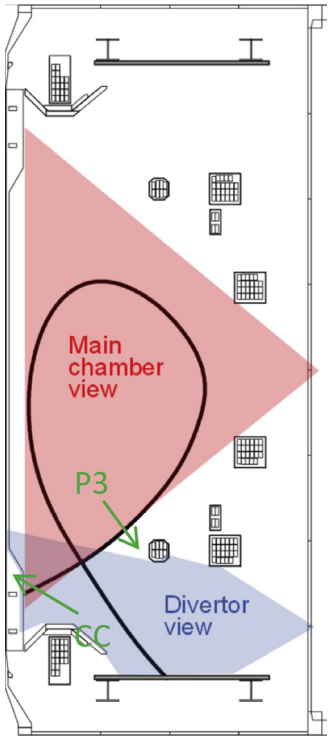

Fig. 1. Viewing geometry of the fast camera in both the main chamber and divertor setup. Note that the view is tangential in real-space. Shown in the figure is a poloidal projection of the view. Highlighted are the P3 poloidal magnetic field coil (P3) and a point on the centre-column (CC).

here is given in Table 1 for the three plasma shots analyzed. Also given is the magnetic field strength, plasma current, line averaged plasma density and safety factor for each of the plasmas.

Plasmas 29,827 and 29,841 are comparable L-mode plasmas in single-null and double-null configurations with a main chamber camera view. Plasma 29,496 is a single-null L-mode and is comparable to 29,827, but with the divertor camera view. Fig. 2 shows a false-color image from the camera for each of these shots, with the geometry of the MAST vessel overlaid to aid perspective.

The movies are processed using a background subtraction technique [14] where a pixel-wise minimum of the 19 preceding frames is subtracted from the current frame. This is motivated by the observation that filaments are positive fluctuations, so the background can be regarded as the minimum of the signal. This method extracts the fluctuating component of the movie allowing for detailed analysis of the filamentary structures.

3. Main chamber view

Fig. 3 presents two series of consecutive frames taken from shots 29,827 and 29,841 which show the evolution of filamentary structures in the main chamber view.

Filaments are clearly visible in the movie frames as elongated structures that wrap around the plasma. They can be seen to follow magnetic field lines [15] and have a small cross-section across the magnetic field. In both sets of frames there is a region where the light intensity maximizes. This is the point at which rays traced from the camera are most tangential to magnetic field-lines, thus maximizing the line-integration of light within the filament.

To infer the presence of filaments across a significant portion of the movie (1800 frames used here) the statistical moments of the pixel-wise time series of the movie are calculated. Fig. 4 shows the mean, standard deviation and skewness of the image intensity calculated for each individual image pixel in shots 29,827 and 29,841.

All three statistical moments maximize on the outboard side towards the upper shoulder of the plasma. In this region the signal is dominated by light emitted in filaments at the tangency angle of the camera with the toroidal direction, therefore the statistical moments measured are representative of a poloidal projection. The poloidal distribution of the moments is strongly affected by the angle between the camera viewing chord and the magnetic field line and maximizes in the upper corner of the plasma. As such poloidal variations are a diagnostic effect whilst radial variations are physical. For the mean and standard deviation the observed poloidal distribution is simply due to increased line-integration through filaments along the camera viewing chord. The skewness variation, which should in principle be independent of line-integration, is slightly subtler. At the point where the camera viewing chord is tangent to magnetic field lines the camera samples a drift-plane and filaments do not overlap one another in the camera view. By contrast, at the outboard midplane multiple filaments that are separate in the drift plane can overlap in the camera view. This causes the distribution in that region to tend towards a Gaussian and reduces the measured skewness. Of the three moments, the skewness is the most appropriate to use for identifying the presence of filaments since it describes how dominant large intermittent events are in the signal. The skewness behaves almost like a halo around the outboard side of the plasmas as filaments are ejected into the SOL. Also shown on the images are projections of the $\psi_N = 1$ and $\psi_N = 1.5$ flux surfaces onto the image at the tangency angle of the camera with the toroidal angle. These surfaces are found to approximately encompass the region of high skewness in both DND and SND. At $\psi_N = 1.5$ magnetic field lines intersect poloidal magnetic field coils within the MAST vessel. This results in a drastic reduction of the connection length within a filament and is likely to quicken drainage of the filament density and

Table 1
Operational parameters of the camera, alongside physical parameters of the plasmas studied here. The spatial resolution quoted is the approximate resolution per-pixel of the camera in the poloidal plane at the camera tangency angle.

Camera parameters				
Shot number	Framerate (kHz)	Exposure time (μs)	Pixel resolution	Spatial resolution
29,841	100	3	160×256	~10mm
29,827	100	3	160×256	~10mm
29,496	120	8	160×192	~5mm
Plasma parameters				
Shot number	I_p(kA)	B_ϕ(T)	$N_{e,LI}(10^{18}m^{-2})$	q_{95}
29,841	415	−0.35	109	5.14
29,827	413	−0.36	91	3.87
29,496	409	−0.46	95	5.26

Please cite this article as: N.R. Walkden et al., Identification of intermittent transport in the scrape-off layer of MAST through high speed imaging, Nuclear Materials and Energy (2016), http://dx.doi.org/10.1016/j.nme.2016.10.024

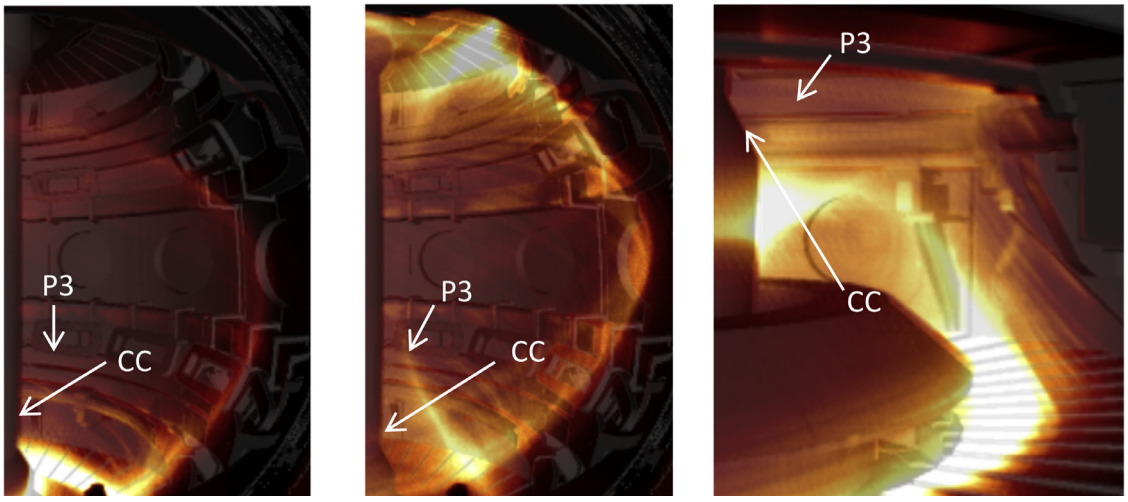

Fig. 2. False-color images taken from movies of shots 29,827 (left), 29,841 (center) and 29,496 (right) overlaid on top of a rendering of the MAST vessel. Features of the image are highlighted which correspond to features in Fig. 1.

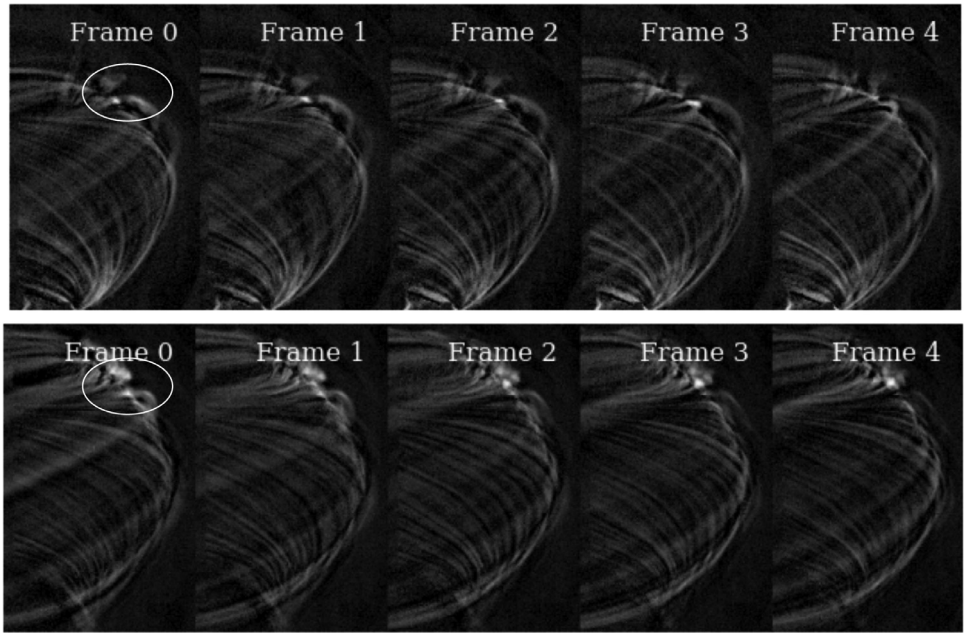

Fig. 3. Sequence of 5 consecutive movie frames from shot 29,827 (upper) and 29,841 (lower) with the background subtraction technique applied. A gamma enhancement with a gamma factor of 0.7 has been applied to aid visual clarity. Circled are regions where the light intensity maximizes, which occur when the camera viewing chord is parallel to the magnetic field.

temperature thereby limiting their propagation and producing the outer boundary observed in the measured skewness. It is notable that in the single null case (29,827) the $\psi_N = 1.5$ flux surface is far outside of the secondary separatrix. By following the path of magnetic fieldlines past the secondary X-point filament shapes become stretched radially and filaments can be observed > 30 cm above the plasma. For single-null machines with a close-fitting wall this effect may lead to excess recycling from the main chamber, as observed in Alcator-C-Mod for example [16]. This effect should also be considered when designing walls for future machines since it may lead to larger than expected wall fluxes away from the outboard midplane.

4. Divertor view

Fig. 5 presents a series of frames from the divertor view in shot 29,496.

As discussed by Harrison et al. [17] there are three distinct regions of filamentary activity present in the divertor. The focus of this paper is on the filamentary activity associated with filaments in the SOL of the outer divertor leg. These are highlighted in Fig. 5. Their shape is distorted by the magnetic field due to shearing and flux-expansion acting on their cross-section [18], similar to that observed just above the X-point by Terry et al. [19].

The statistical analysis conducted in the previous section has now been applied to the divertor view of the camera. Once again regions where the signal is dominated by the light emission at the tangency angle can be considered as approximate poloidal projections of the statistical moments. This is the case for the outer divertor leg region under study here. The statistical moments of the movie for shot 29,496 are shown in Fig. 6.

In the divertor view filaments are observed as an area of high mean, variance and skewness outside the outer divertor leg (right hand side of the image). The peak skewness observed above the

Please cite this article as: N.R. Walkden et al., Identification of intermittent transport in the scrape-off layer of MAST through high speed imaging, Nuclear Materials and Energy (2016), http://dx.doi.org/10.1016/j.nme.2016.10.024

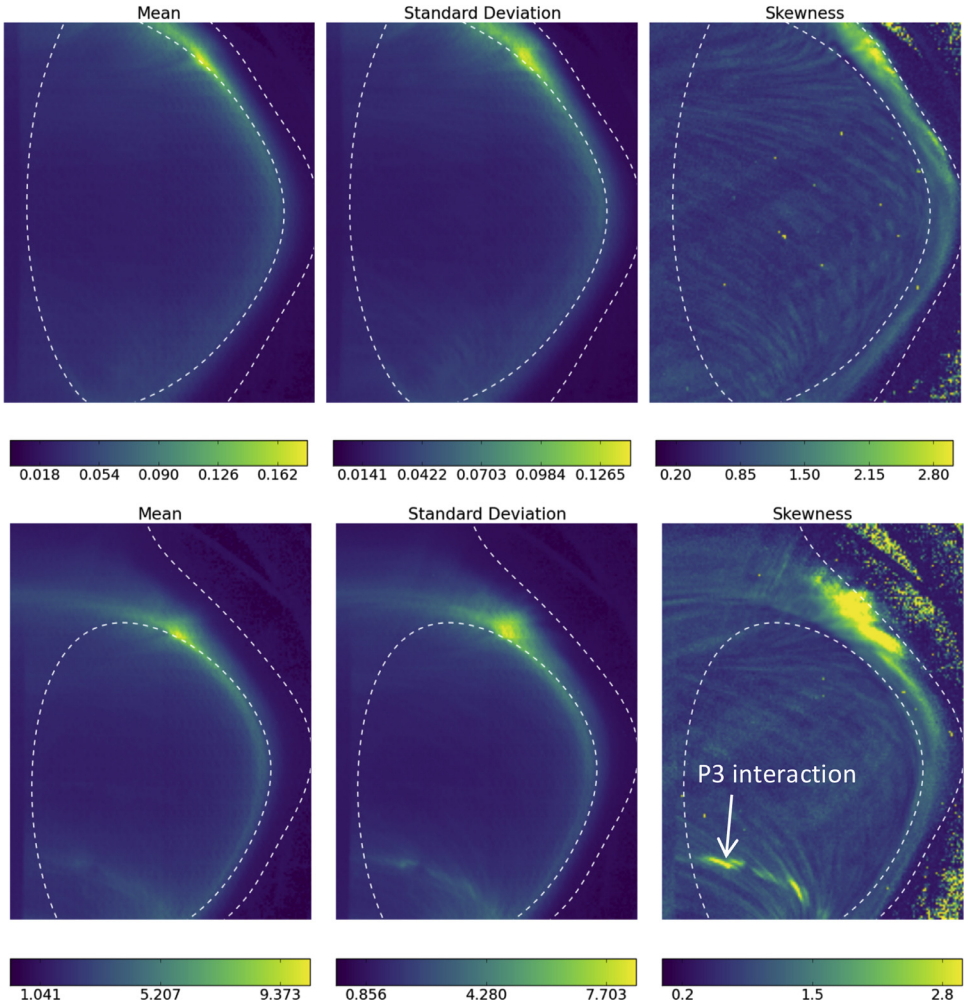

Fig. 4. Pixel-wise mean (left), standard deviation (center) and skewness (right) for shot 29,841 (upper) and 29,827 (lower). Overlaid are projections of the $\psi_N = 1$ and $\psi_N = 1.5$ flux surfaces onto the image. These flux surfaces encompass the regions of higher skewness which are indicative of the presence of filaments. High levels of skewness are present outside of this region with an apparently random distribution. In this region the camera view is blocked by the viewing port geometry so only noise is picked up by the camera and the resulting skewness measured in this noise can be neglected.

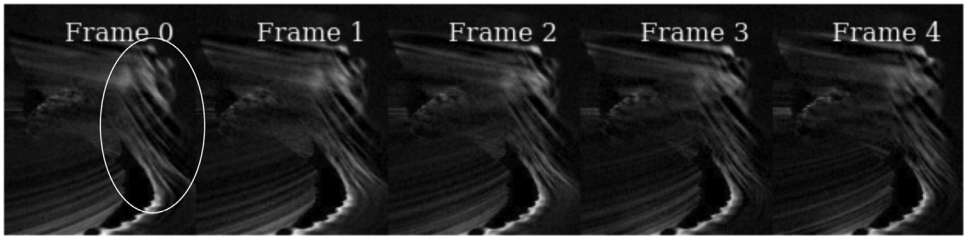

Fig. 5. Frame sequence from shot 29,496 showing elongated filamentary structures in the SOL region. A gamma enhancement with a gamma factor of 0.7 has been applied for visual clarity. Highlighted in frame 0 are the filaments of interest for this study.

X-point in the inner leg occurs as the plasma interacts with the P3 poloidal field coil and is not of interest here. There is a significant region between the flux surfaces $\psi_N = 1$ and $\psi_N = 1.03$ where all three statistical moments drop. This region coincides with a close proximity to the X-point. The drop in skewness indicates that there are few identifiable filaments in this region. This can be further verified by measuring the signal intensity along a line of interest (LOI) which originates at the X-point and spans radially outward, as shown in Fig. 7.

Fig. 7 shows a clear change in nature of fluctuations that cross the LOI inside $\psi_N = 1.03$. Outside of this flux surface the light measured by the camera is dominated by line-integration through the filament cross-section at the tangency radius (i.e measuring the poloidal cross-section of the filament). Inside of $\psi_N = 1.03$ the only contribution to the light is from filaments passing in front or behind the plasma, indicating that there are no identifiable filaments in the region in the poloidal plane. The cause of this cutoff is presently uncertain but is likely to be related to the shearing effect of the magnetic field on the filament cross-section [18]. Also shown in Fig. 7 is the magnetic shear integrated from the outboard midplane to the LOI. The magnetic shear increases rapidly beyond $\psi_N = 1.03$ which will cause an extreme lengthscale contraction in filaments that occupy this region [20,21]. This lengthscale contraction may cause enhanced dissipation in the filament [21] or result

Please cite this article as: N.R. Walkden et al., Identification of intermittent transport in the scrape-off layer of MAST through high speed imaging, Nuclear Materials and Energy (2016), http://dx.doi.org/10.1016/j.nme.2016.10.024

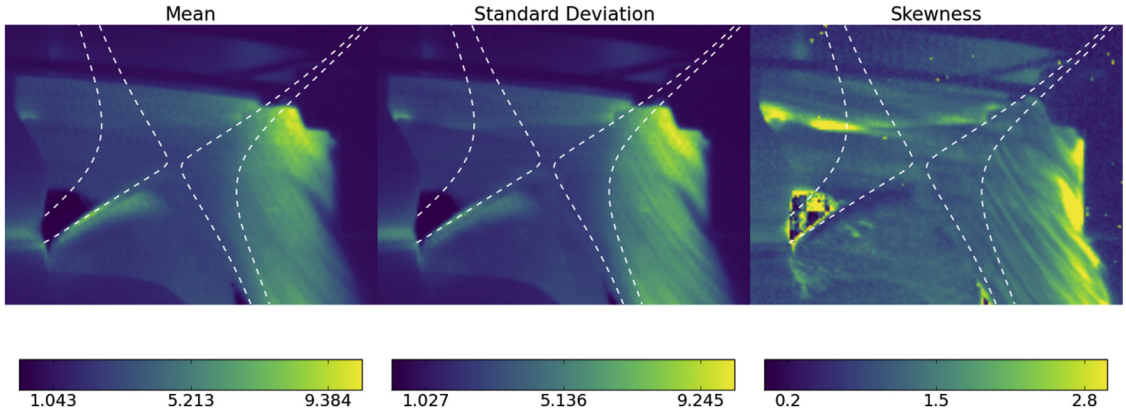

Fig. 6. Pixel-wise mean (left), standard deviation (center) and skewness (right) in the divertor camera view for shot 29,496. Shown in the diagrams are projections of the $\psi_N = 1$ and $\psi_N = 1.03$ flux surfaces which encompass a region close to the X-point that is devoid of filaments. The drop in the mean and standard deviation close to the inner strike point is due to saturation of the camera sensor, which combined with background subtraction, suppresses these quantities in that region. There is also a sharp change in the statistical moments to the far right hand side of the view due to the blocking of light from the plasma by a poloidal field coil support structure.

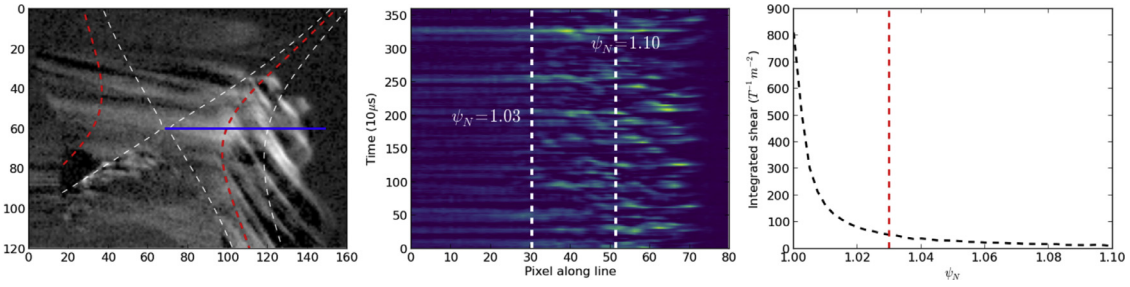

Fig. 7. Left: Divertor view image showing LOI position (blue line) the separatrix (white, inner), $\psi_N = 1.03$ (red) and $\psi_N = 1.1$(white, outer) flux surfaces. Centre: Signal intensity along the LOI over 350 frames of the movie. Right: Magnetic shear, integrated from the midplane to the LOI showing a steep rise inside $\psi_N = 1.03$. (For interpretation of the references to colour in this figure legend, the reader is referred to the web version of this article.)

in blurring of filaments together in the camera view. It may also contribute to the observed decorrelation of fluctuations at the divertor target with upstream fluctuations in NSTX [22]. Indeed such a decorrelation close to the separatrix has been predicted in modelling conducted with the BOUT code [23] as a result of the proximity to the X-point. A fuller investigation of the causes of the quiescent X-point region will appear in a future paper.

The observations above may be significant given that the peak heat flux to the divertor is delivered in this region of flux-space. It is therefore important to understand how filaments are being denatured in this region so that the nature of the heat flux that is delivered to the target can be understood.

5. Summary

This paper presents a study of intermittent transport phenomena called filaments in the MAST SOL using high speed imaging with tangential views of both the main chamber and divertor volumes. In the main chamber view double and single-null magnetic configurations have been analyzed and filaments are found to propagate up to and beyond the $\psi_N = 1.5$ magnetic flux-surface. In the SND case this surface lies outside the secondary separatrix and, through interaction with the secondary X-point, leads to the identification of filaments > 30 cm above the plasma. The implications of such a large region of filamentary activity should be considered in the context of close-fitting first-walls for future machines.

In the divertor view filaments are observed in the SOL of the outer divertor leg. In the vicinity of the X-point a region is present between the flux surfaces $\psi_N = 1$ and $\psi_N = 1.03$ where the plasma is quiescent and no coherent filaments are identified. The cause of this is presently uncertain, however it is likely that magnetic shear, which is shown to increase sharply within the region of quiescence, can denature the filaments and possibly contribute to their loss of coherency. It will be important to understand this process given its role in determining heat fluxes to the divertor target.

Acknowledgments

We gratefully acknowledge many useful conversations with Dr D Moulton. This work has been carried out within the framework of the EUROfusion Consortium and has received funding from the Euratom research and training programme 2014–2018 under grant agreement No 633,053 and from the RCUK Energy Programme [grant number EP/I501045]. To obtain further information on the data and models underlying this paper please contact PublicationsManager@ccfe.ac.uk. The views and opinions expressed herein do not necessarily reflect those of the European Commission.

References

[1] P.C. Stangeby, The Plasma Boundary of Magnetic Fusion Devices, IOP Publishing Ltd, London, UK, 2000.
[2] B. Lipschultz, et al., Nucl. Fusion 47 (2007) 1189.
[3] R.P. Wenninger, et al., Nucl. Fusion 54 (2014) 114003.
[4] O.E. Garcia, et al., J. Nucl. Mater. 363-365 (2007) 575.
[5] A. Kirk, et al., Plasma Phys. Control. Fusion 48 (2006) B433.
[6] R.J. Maqueda, et al., Rev. Sci. Instrum. 72 (2001) 931.
[7] B. Nold, et al., Plasma Phys. Control. Fusion 52 (2010) 065005.
[8] N. Katz, et al., Phys. Rev. Lett. 101 (2008) 015003.
[9] T. Happel, et al., Phys. Rev. Lett. 102 (2009) 255001.
[10] G.Y. Antar, et al., Phys. Plasmas 10 (2003) 419.
[11] A. Thornton, G. Fishpool, A. Kirk, Plasma. Phys. Control. Fusion 57 (2015) 115010.
[12] A. Kirk, et al., Plasma Phys. Control. Fusion (2016) https://arxiv.org/abs/1602.03021.
[13] S.Y. Allan, et al., Plasma Phys. Control. Fusion 58 (2016) 045014.

Please cite this article as: N.R. Walkden et al., Identification of intermittent transport in the scrape-off layer of MAST through high speed imaging, Nuclear Materials and Energy (2016), http://dx.doi.org/10.1016/j.nme.2016.10.024

[14] B.D. Dudson, Edge Turbulence in the Mega Amp Spherical Tokamak PhD Thesis, University of Oxford, 2007.
[15] N.B. Ayed, et al., Plasma Phys. Control. Fusion 51 (2009) 035016.
[16] M.V. Umanksy, et al., Phys. Plasmas 5 (1998) 3373.
[17] J. Harrison, et al., J. Nucl. Mater. 463 (2014) 757.
[18] D. Farina, et al., Nucl. Fusion 33 (1993) 9.
[19] J. Terry, et al., J. Nucl. Mater. 390–391 (2009) 339–342.
[20] J.R. Myra, et al., Phys. Plasmas 13 (2006) 112502.
[21] N.R. Walkden, Properties of Intermittent Transport in the Mega Ampere Spherical Tokamak PhD Thesis, University of York, 2015.
[22] R.J. Maqueda, et al., Nucl. Fusion 50 (2010) 075002.
[23] M.V. Umanksy, et al., J. Nucl. Mater. 337–339 (2005) 266–270.

Please cite this article as: N.R. Walkden et al., Identification of intermittent transport in the scrape-off layer of MAST through high speed imaging, Nuclear Materials and Energy (2016), http://dx.doi.org/10.1016/j.nme.2016.10.024